High resolution threshold photoelectron spectrum of oxygen in the 12–19 eV region

T. Akahori, Y. Morioka, T. Tanaka, H. Yoshii, T. Hayaishi, and K. Ito

Citation: The Journal of Chemical Physics **107**, 4875 (1997); doi: 10.1063/1.474849
View online: http://dx.doi.org/10.1063/1.474849
View Table of Contents: http://scitation.aip.org/content/aip/journal/jcp/107/13?ver=pdfcov
Published by the AIP Publishing

High resolution threshold photoelectron spectrum of oxygen in the 12–19 eV region

T. Akahori
Sumitomo Metal Industries Ltd., Amagasaki, Hyogo 660, Japan

Y. Morioka, T. Tanaka, and H. Yoshii
Institute of Physics, University of Tsukuba, Tsukuba, Ibaraki 305, Japan

T. Hayaishi
Institute of Applied Physics, University of Tsukuba, Tsukuba, Ibaraki 305, Japan

K. Ito
National Laboratory for High Energy Physics, Oho, Tsukuba, Ibaraki 305, Japan

(Received 18 November 1996; accepted 19 June 1997)

The threshold photoelectron spectrum of oxygen has been measured with high resolution in the photon energy range of 12–19 eV using a penetrating field technique and a synchrotron radiation source. The long vibrational progression of the $X^2\Pi_g$ state of O_2^+ was observed to $v'=45$. An extrapolation in a Birge–Sponer plot (ΔG versus $v'+1/2$) gives a maximum vibrational level $v'_{\max}=56$. The $A^2\Pi_u$ state was also measured in detail. Most vibrational levels of the $A^2\Pi_u$ state of O_2^+ (from $v'=0$ to 24) were observed for the first time. A Birge–Sponer plot of the $A^2\Pi_u$ state gives a maximum vibrational level $v'_{\max}=31$. The dissociation limit of the $A^2\Pi_u$ state is slightly higher (76 meV) than the well-known dissociation limit $O(^3P_2)+O^+(^3S_0)$ 18.733 eV. Therefore the $A^2\Pi_u$ state may be considered to have a hump. We observed new states which were assigned to $^4\Sigma_g^+$ and $^2\Sigma_u^+$ according to a previous theoretical investigation [Beebe *et al.*, J. Chem. Phys. **64**, 2080 (1976)]. Potential curves of the $X^2\Pi_g$ and $A^2\Pi_u$ states were calculated by the Rydberg–Klein–Rees method using both the rotational constants obtained previously by others [K. P. Huber and G. Herzberg, *Molecular Spectra and Molecular Structure*, Constants of Diatomic Molecules Volume IV (Van Nostrand, New York, 1974)] and the vibrational energy values observed in the present experiment. A Le Roy–Bernstein plot as well as a Birge–Sponer plot were used to determine the dissociation energy of the $X^2\Pi_g$ state. However, the plot gave an unreasonably large dissociation limit. © *1997 American Institute of Physics.* [S0021-9606(97)01036-2]

I. INTRODUCTION

Ionic states of O_2 have been studied by many investigators and many states have been precisely identified. The exact ionization energies of O_2 have been indirectly determined by deducing the series limits of Rydberg states, or by adding the excitation energy to that of the lower state or subtracting the excitation energy from that of the higher state. Photoelectron spectroscopy can determine the ionization energies directly but not so exactly because photoelectron spectroscopy usually has a resolution of more than 10 meV. Edqvist *et al.*[1] measured the photoelectron spectrum (PES) of O_2 in the range of 12–28 eV with 584 and 304 Å He resonance lines. Samson and Gardner[2] measured the vibrational levels up to about $v'=25$ of the $X^2\Pi_g$ state of O_2^+ using Ne resonance lines. Higher vibrational levels ($v'>20$) of the ground $X^2\Pi_g$ state of O_2^+ overlap with lower vibrational levels of the $a^4\Pi_u$ state of O_2^+ and also their photoelectron intensity may be predicted to be very weak due to the smallness of their Franck–Condon factors from the ground state of O_2. Therefore, it was difficult to identify high vibrational levels ($v'>20$) of the $X^2\Pi_g$ state of O_2^+. Merkt and Guyon[3] observed spin-orbit components $^2\Pi_{1/2}$ and $^2\Pi_{3/2}$ of the vibrational levels of the ground state up to $v'=26$ by threshold photoelectron spectroscopy (TPES) with high resolution.

The vibrational levels of the $A^2\Pi_u$ state overlap those of the $a^4\Pi_u$ state as well as of the $X^2\Pi_g$ state and an accurate measurement of the higher vibrational energy levels of the $A^2\Pi_u$ state has not been performed, though the emission measurement of the transition to the $X^2\Pi_g$ state from the $A^2\Pi_u$ state, which is called the second negative band, was performed in the lower vibrational levels by many investigators (see, e.g., Ref. 4). Edqvist *et al.*[1] measured the $A^2\Pi_u$ state in the photoelectron spectrum of oxygen. In their experiment, the resolution was about 12 meV (halfwidth) as measured for the $Ar(3p)^{-1}$ doublet. Since the spectrum of the $a^4\Pi_u$ state of O_2^+ had a broad feature with a 26 meV halfwidth, while the spectra of the $A^2\Pi_u$ and $b^4\Sigma_g^-$ states had a 16 meV halfwidth, they predicted that the broadness was due to the quartet structure which could not be resolved by their experimental conditions. Deconvolution was carried out between the vibrational levels $v'=5$, 9 of the $A^2\Pi_u$ state and $v'=13$,17 of the $a^4\Pi_u$ state, respectively. Morioka *et al.*[5] observed by using a supersonic jet and a time-of-flight spectrometer that the spectra of the $v'=1$ to 6 levels of the $a^4\Pi_u$ state are split into four components as predicted from the quartet multiplicity of that state. TPES has the characteristic that it is strongly affected by autoionization in contrast to PES in which intensity is mainly determined by Franck–

Condon factors. Therefore, if a vibrational level of an ionic state coincides with an autoionization state which has an appropriate absorption cross section from the ground state, the TPES signal of the level may be observed even if the Franck–Condon factor for the direct PES transition is too small.

Configuration interaction calculations of low-lying electronic states of O_2^+ were reported by Beebe *et al.*[6] They suggested that in addition to the $X^2\Pi_g$, $A^2\Pi_u$ and $a^4\Pi_u$ states, four other bound states which dissociate to the first dissociation limit are possible, that is, $^2\Sigma_u^+$, $^4\Sigma_g^+$, $^6\Sigma_u^+$ and $^4\Pi_g$, and they gave predicted spectroscopic constants (T_e, r_e, w_e, D_e) of these states. Yeager *et al.*[7] calculated the ionization energies and the potential curves of seven lower states of O_2^+. They argued the $A^2\Pi_u$ state dissociates diabatically to the third limit, though it is usually considered to dissociate (adiabatically) to the first limit. However, their value of $w_e(A^2\Pi_u)=2133.2\ \mathrm{cm}^{-1}$ disagrees very badly with experiment ($w_e=894\ \mathrm{cm}^{-1}$).

In the present work, we observed the TPES of O_2 in the 12–19 eV region, and obtained nearly complete vibrational progressions of the X, a and A states of O_2^+. We were able to obtain the corresponding potential curves of the X and A states by using the Rydberg–Klein–Rees (RKR) method.[8–11]

II. EXPERIMENTAL METHOD

The experimental method was described previously by Lu *et al.*[12,13] and will be reviewed briefly in this section. Threshold photoelectrons were detected by a penetrating field electrostatic analyzer. The light source was supplied by a high-flux 3 m normal incidence monochromator installed at beam line 20A of the Photon Factory, National Laboratory for High Energy Physics, Tsukuba.[14] A photon bandwidth of 0.03 Å was obtained with 15 μm slits and 2400 lines/mm grating. The oxygen gas was cooled by supersonic expansion through a 30-μm-diam nozzle and a stagnation pressure of approximately 4 atm. The vacuum chamber was evacuated with a cryopump which has a pumping speed of 20 000 ℓ/s and which maintained a background pressure of 1×10^{-5} Torr in the presence of the gas beam. The nozzle was located at a distance of about 10 mm from the ionization region.

The threshold photoelectron analyzer and the ion monitor which was located on the opposite side of the analyzer were mounted with a separation of 33 mm and the photon beam intersected the gas beam perpendicularly. Electrons extracted by the penetrating field were focused and discriminated by the chromatic aberration of the lens system and then analyzed by a hemispherical analyzer to eliminate hot electrons which pass directly through the lens system. The threshold electron spectrum was obtained by setting the hemispherical analyzer to collect zero kinetic energy electrons and scanning the photon wavelength. The energy resolution of the threshold electron analyzer was estimated to be under half a meV by measuring the threshold electron spectrum of the Xe first ionization limit at 1022.1 Å where the energy resolution of the monochromator was much better than in the shorter wavelength regions. The energy resolution

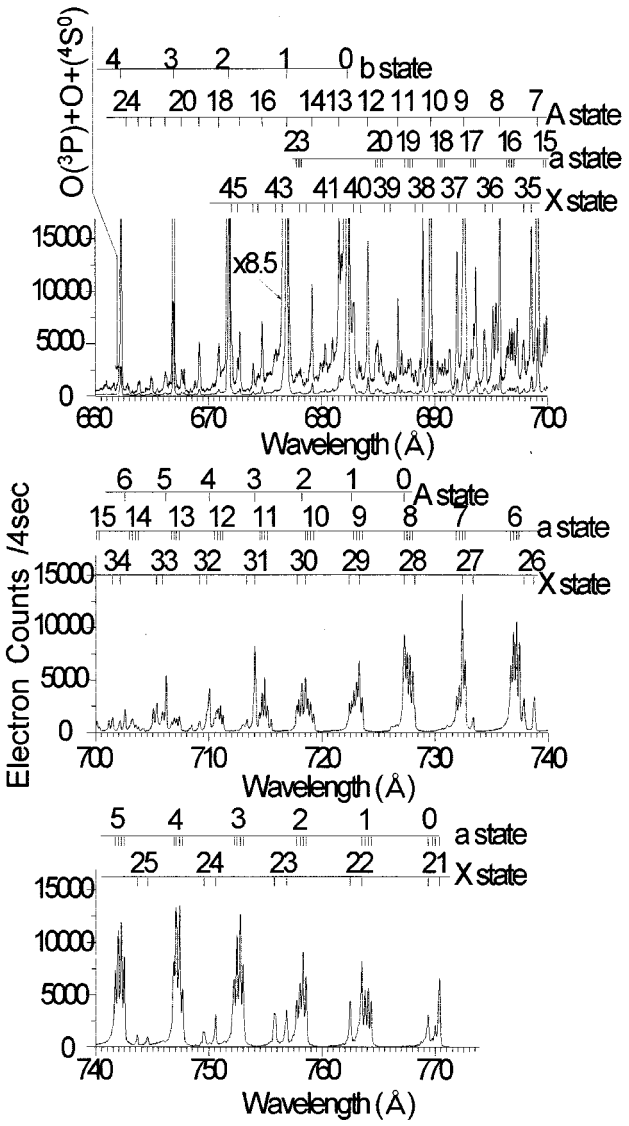

FIG. 1. A threshold photoelecton spectrum of O_2^+ between 660 and 775 Å.

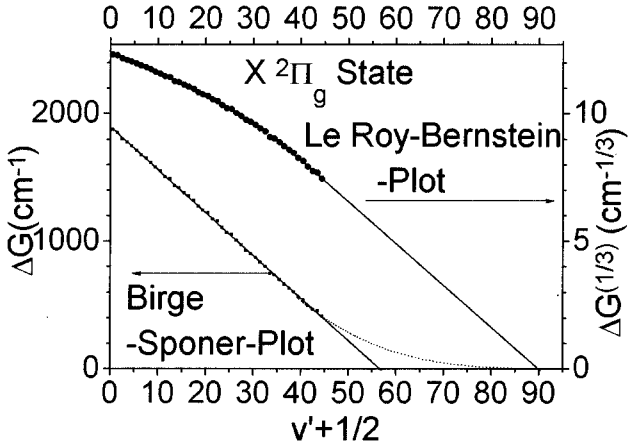

FIG. 2. A Birge–Sponer plot of the $X^2\Pi_g$ state of O_2^+. The curve is obtained by the least squares method. A Le Roy–Bernstein plot is also shown (see the text). The dashed curve presents a ΔG versus $(v'+1/2)$ curve using parameters obtained by the Le Roy–Bernstein plot.

TABLE I. Vibrational constants of the $X^2\Pi_g$ state.

Molecular constant	Present data (cm^{-1})	Photoelectron spectroscopy		Spectroscopic data	
		Samson and Gardner[a]	Edqvist *et al.*[b]	Krupenie[c]	Bhale and Rao[d]
T_e	96 472.3±7.3				
ω_e	1 917.8±0.7	1910±25	1905±7	1905±2	1903.85
$\omega_e x_e$	16.92±0.02	16.67±0.3	16.6±0.5	16.28±0.12	16.18

[a]Reference 2.
[b]Reference 1.
[c]Reference 15.
[d]Reference 16.

with the same slit widths of the monochromator degraded with shortening wavelength and therefore became about 1 meV in the 700 Å region and 2 meV in the 500 Å region. The wavelength was scanned in steps of 0.02 Å, typically, and the spectra were obtained with dwell times of 4 s/step. The wavelength calibration, and hence the energy calibration was performed by measuring the autoionizing peaks of rare gases.

III. RESULT AND DISCUSSION

Figure 1 shows part of the threshold photoelectron spectrum obtained in the present experiment from 660 to 770 Å, though we have observed to 1023 Å, which is the location of $v'=0$ of the ground $X^2\Pi_g$ of O_2^+, from the first dissociation limit $(O(^3P)+O^+(^4S_0))$ of the X, a, and A states at 661.85 Å. The vibrational levels of the X, a and A states are indicated by vertical ticks. We will discuss these states separately and new states at the end.

A. The $X^2\Pi_g$ state

The doublet structure of the $X^2\Pi_g$ state is confirmed in Figure 1. The vibrational progression of the state is observed to $v'=45$. A Birge–Sponer plot, which is a plot of the separation of successive levels ΔG versus $(v+1/2)$, is shown in Figure 2 (using the average of $J=1/2$ and 3/2 components of observed term value $G(v)$), and a least squares fit to the data is also shown by the solid line. An extrapolation of the present ΔG to zero gives a maximum vibrational level $v'_{max}=56$, which agrees with the data of Samson and Gardner,[2] who determined the maximum vibrational level $v'_{max}=56.5$ from a linear extrapolation of ΔG from $v'=0$ to 25. The w_e and $w_e x_e$ of the $X^2\Pi_g$ state of O_2^+ are indicated in Table I and compared with other data previously observed.[1,2,15,16] The small difference from other data comes from the fact that the present data were calculated using the energy values of higher vibrational levels ($v'=45$) with respect to other data's vibrational levels ($v'<25$) to the least square method. The energy of the maximum vibrational level ($v'_{max}=56$) obtained by the least squares method is 18.699 ±0.001 eV, which is lower than the first dissociation limit $(O(^3P)+O^+(^4S_0))$ (18.733±0.003 eV)[17] by 34 meV±4.

A Le Roy–Bernstein plot[18] was used to try to obtain a more reliable dissociation limit. The plot is shown in Figure 2 with the Birge–Sponer plot. If we assume the last number of the vibrational quantum number should be 90 and the cubic root of ΔG is linear in $v'+1/2$, we can obtain the value 18.975±0.035 eV as the dissociation limit, which we think is too much larger than the well-known value 18.733 ±0.003 eV. It is considered that higher vibrational states near the dissociation limit are necessary for analysis by a Le Roy–Bernstein plot.

The potential curve of the $X^2\Pi_g$ state was calculated using the RKR method[8–11] on the basis of the data obtained

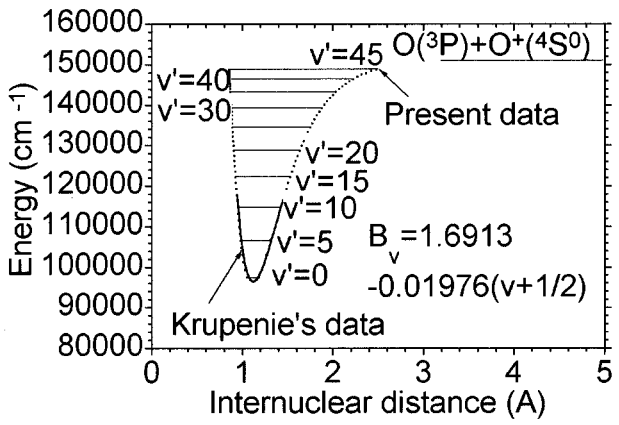

FIG. 3. The potential curve of the $X^2\Pi_g$ state of O_2^+ obtained in the present experiment and by Krupenie.

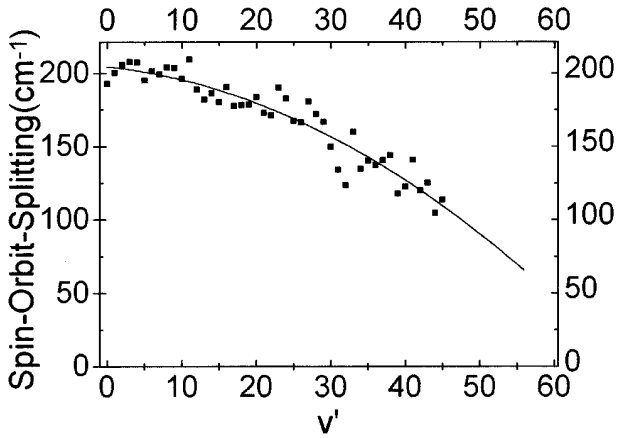

FIG. 4. The spin-orbit-splitting of the $X^2\Pi_g$ state of O_2^+ versus v'.

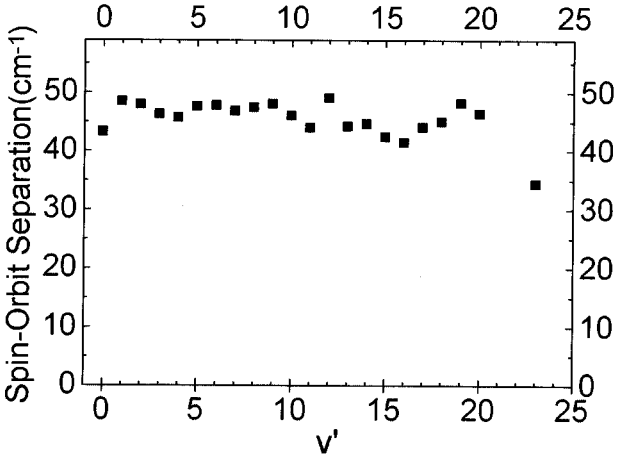

FIG. 5. The spin-orbit-splitting of the $a^4\Pi_u$ state of O_2^+ versus v'.

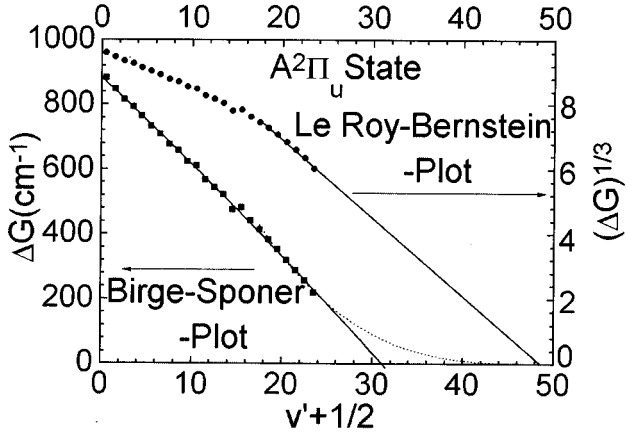

FIG. 7. A Birge–Sponer plot of the $A^2\Pi_u$ state of O_2^+. The solid curve was obtained by the least squares method. A Le Roy–Bernstein plot is also shown (see the text). The dashed curve presents a ΔG versus $(v'+1/2)$ curve using parameters obtained by the Le Roy–Bernstein plot.

in the present experiment and the rotational constants obtained previously by others[17] and shown in Figure 3. The potential curve of O_2^+ was obtained previously by Krupenie[15] and is also shown in Figure 3 by a solid line. Singh and Rai[19] calculated the potential curve of this state and their data agree with ours as well as that of Krupenie, which is not shown because they showed only the lower vibrational levels and because they agree exactly with ours.

The spin-orbit splitting of the $X^2\Pi_g$ was measured to $v'=45$ and is shown in Figure 4. The curve of these splittings is predicted to converge to zero, approaching the dissociation limit, because the lowest dissociation limit $(O(^3P_2)+O^+(^4S_0))$ is connected with 10 gerade and ungerade molecular states and the $X^2\Pi_g$, $A^2\Pi_u$ and $a^4\Pi_u$ states dissociate to the same lowest $^3P_2$ state due to the non-crossing rule, if the non-crossing rule exactly holds. As you can see, the magnitude of the observed splitting seems to approach zero. The best fit curve of the variation of the magnitudes versus v' is also shown with a solid line in the figure.

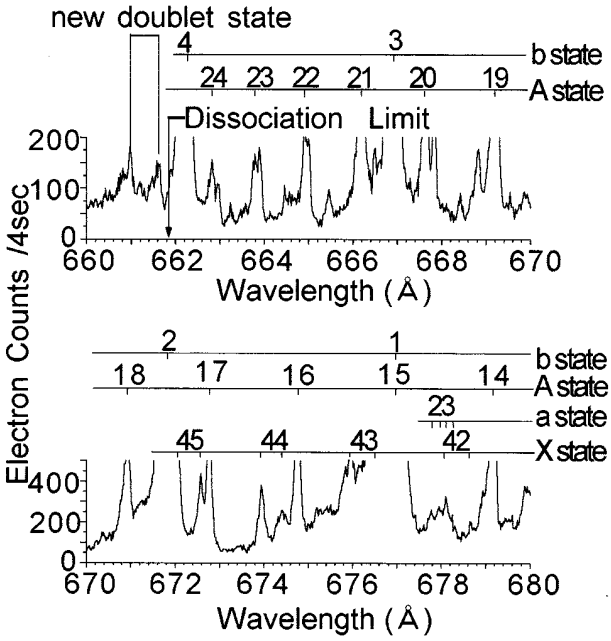

FIG. 6. The threshold electron spectrum of O_2^+ near the first dissociation limit.

B. The $a^4\Pi_u$ state

The spectrum of the $a^4\Pi_u$ state can be seen in Figure 1 and the quartet structure is clearly separated. This structure was already observed in the threshold photoelectron spectrum by Morioka *et al.*[5] and optically by Nevin.[20] The present result is a higher resolution than that observed by Morioka *et al.*[5] The average of the spin-orbit splitting versus v' is plotted in Figure 5. However, the four spin-orbit splitting levels of the $a^4\Pi_u$ state must reach the $^3P_2$ state of the O atom for the reason mentioned in Section III A. The variation versus v' is not recognized in the region of this figure. The drastic decrease of spin-orbit splitting near the dissociation limit is predicted.

C. The $A^2\Pi_u$ state

Detailed measurement of the $A^2\Pi_u$ state has been difficult due to overlapping higher levels of the $a^4\Pi_u$ state. In

TABLE II. Vibrational constants of the $A^2\Pi_u$ state.

Molecular constant	Present data	Photoelectron data[a]	Spectroscopic data	
T_e	137 069±8	17.045 eV	40 669[b]	
ω_e	894.4±2.8	896±4	898.2±0.5[b]	895.59[c]
$\omega_e x_e$	12.96±0.26	13.1± 0.2	13.57±0.03[b]	13.15[c]
$\omega_e y_e$	−0.021±0.007			

[a]Reference 1.
[b]Reference 15.
[c]Reference 16.

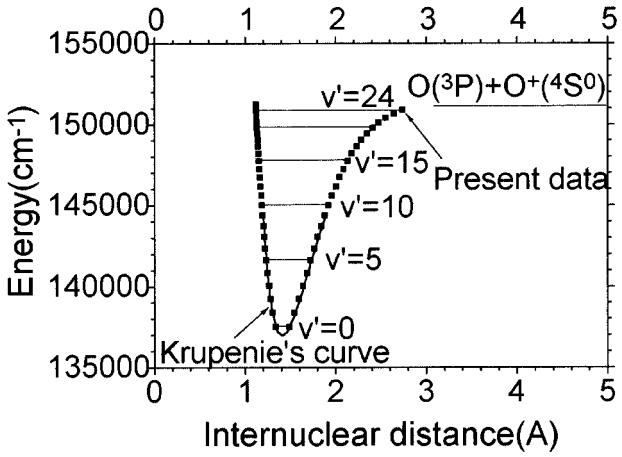

FIG. 8. The potential curve of the $A^2\Pi_u$ state of O_2^+ obtained in the present experiment and by Krupenie (see Ref. 15).

addition, the $A^2\Pi_u$ state becomes weaker as it gets closer to the dissociation limit in the case of photoelectron spectroscopy. We also tried to measure the $A^2\Pi_u$ state by TPES with high resolution. The long vibrational progression of the $A^2\Pi_u$ state was observed as can be seen in Figure 6. A Birge–Sponer plot of the $A^2\Pi_u$ state is shown in Figure 7. A least squares fit of a polynomial approximation for ΔG in the plot can be seen to be quite smooth. An extrapolation of ΔG to zero gives both a maximum vibration level $v'_{\max}=31$ and a dissociation limit 18.809 ± 0.006 eV. This dissociation limit is higher than the first dissociation limit $O(^3P_2)+O^+(^4S_0)$ 18.733 ± 0.003 eV. It is recognized from this result that the potential curve of the $A^2\Pi_u$ state has a small potential hump ($18.809\pm0.006-18.733\pm0.003$ eV$=76\pm7$ meV) above the dissociation limit ($O(^3P_2)+O^+(^4S_0)$), because we cannot adopt the second dissociation limit instead of that, considering the energy gap between these limits. Molecular constants obtained in the present experiment are shown in Table II.

If the potential curve has a hump, the reason will be the existence of the mixing of the states. In that case, a Le Roy–Bernstein plot will not work to obtain the exact dissociation limit and the final vibrational quantum number, though the plot is shown in Figure 7 as well as a Birge–Sponer plot and gave 18.900 ± 0.007 eV as the dissociation energy.

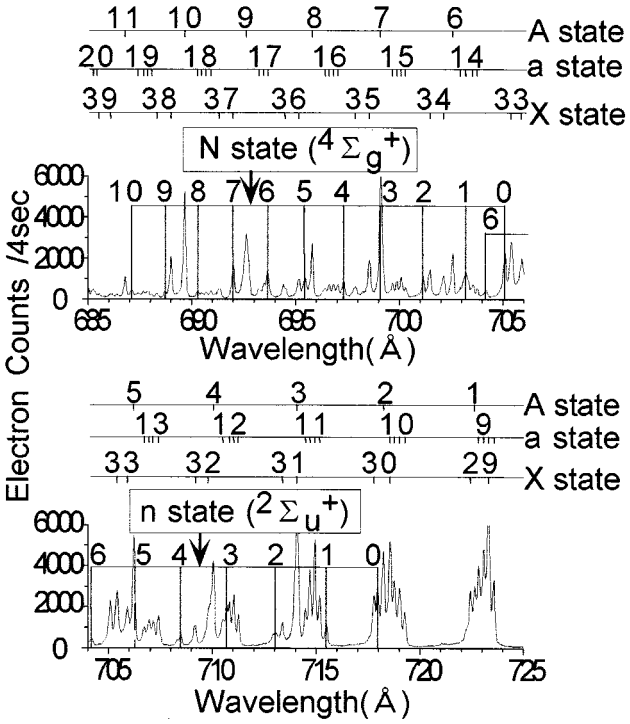

FIG. 9. The threshold electron spectrum of the new states.

A potential curve of the $A^2\Pi_u$ state calculated in the present work by using the RKR method is shown in Figure 8 and the potential curve by Krupenie[15] is also shown by a solid line.

D. New states

We observed two new states. Figure 9 shows the observed threshold photoelectron spectrum in wavelength region from 685 to 725 Å. Two new states are labeled by *n* and *N* (*n* and *N* mean new states) and marked above the peaks

TABLE III. Wavelengths and wavenumbers of new states.

n state				*N* state		
Vibrational number	Wavelength (A)	Wave number (cm^{-1})	Separation (cm^{-1})	Wavelength (A)	Wave number (cm^{-1})	Separation (cm^{-1})
0	717.95	139285	479	705.08	141828	379
1	715.49	139764	482	703.20	142207	422
2	713.03	140247	464	701.12	142629	414
3	710.68	140710	439	699.09	143043	365
4	708.47	141149		697.31	143408	390
5				695.42	143798	367
6	704.16	142013		693.65	144165	348
7				691.98	144513	356
8				690.28	144869	330
9				688.71	145199	340
10				687.10	145539	

TABLE IV. Molecular constants of new states.

State	Molecular constants	Present data (cm^{-1})	Predicted (Beebe *et al.*)
	ω_e	499.5±4.3	607
	$\omega_e x_e$	6.37±0.60	
n state ($^4\Sigma_g^+$)	T_e	139285(17.269 eV)	12.07+5.37=17.44 eV
	D_e	9792(1.21 eV)	
	T_e+D_e	149077(18.483 eV)	
	ω_e	419.9±3.1	522
	$\omega_e x_e$	4.41±0.27	
N state ($^2\Sigma_u^+$)	T_e	141579(17.554 eV)	12.07+5.81=17.88 eV
	D_e	9991(1.24 eV)	
	T_e+D_e	151570(18.792 eV)	

with the predicted vibrational quantum number (for example, 0,1,2,...,). Wavelengths of the *n* and *N* states are shown in Table III. By predicting the Morse potential function and therefore, using a second-degree polynomial fit of these data, $w_e, w_e x_e$, the term value T_e and the dissociation energy D_e were calculated and are shown in Table IV. The calculated dissociation limits (T_e+D_e) of the *n* and *N* states are 18.483 and 18.792 eV, respectively. These dissociation limits, especially in the case of the *N* state, are very close to the predicted dissociation limit ($O(^3P)+O^+(^4S_0)$) 18.733 eV. Possible states which may arise from this limit are $^{2,4,6}\Sigma_{g,u}^+$, $^{2,4,6}\Pi_{g,u}$. The potential energy curves for these states were calculated by Beebe *et al.*[6] The $^4\Pi_g$ state has been well investigated by many authors.[21–25] We cannot recognize, in the present experiment, the $^4\Pi_g$ state which is predicted to have a shallow minimum. It is assumed here that these new states *n* and *N* are the $^4\Sigma_g^+$ and $^2\Sigma_u^+$ states, respectively, comparing these vibrational constants and energies with the data predicted by Beebe *et al.*[6] However, the possibility remains that these vibrational structures belong to $^6\Sigma_u^+$ or $^4\Pi_g$. In the future, characteristics of these new states will be clarified by aid of more precise calculation.

IV. SUMMARY

We have reported the high resolution threshold photoelectron spectra of the $X^2\Pi_g$, $a^4\Pi_u$ and $A^2\Pi_u$ states of O_2^+. The doublet structure of the $X^2\Pi_g$ and the quartet structure of the $a^4\Pi_u$ state were observed. The long vibrational progressions were observed up to the $v'=45$ and $v'=24$ for the $X^2\Pi_g$, and $A^2\Pi_u$ states, respectively. The potential curve of the *A* state has a small potential barrier (76 meV) above the dissociation limit ($O(^3P)+O^+(^4S_0)$). In addition, we could observe the $^4\Sigma_g^+$ and $^2\Sigma_u^+$ states directly for the first time.

ACKNOWLEDGMENTS

We are grateful to the staff of the National Laboratory for High Energy Physics for experimental support. This research work was performed at the Photon Factory under Contract No. 95G-408.

[1] O. Edqvist, E. Lindholm, L. E. Selin, and L. Åsbrink, Phys. Sc. **1**, 25 (1970).
[2] J. A. R. Samson and J. L. Gardner, J. Chem. Phys. **67**, 755 (1977).
[3] F. Merkt, P. M. Guyon, and J. Hepburn, Chem. Phys. **173**, 479 (1993).
[4] D. L. Albritton, W. J. Harrop, and A. L. Schmeltekopf, J. Mol. Specrosc. **46**, 89 (1973).
[5] Y. Morioka, Y. Lu, T. Matsui, K. Ito, and Hayaishi, J. Phys. B **26**, L535 (1993).
[6] N. H. F. Beebe, E. W. Thulstrup, and A. Andersen, J. Chem. Phys. **64**, 2080 (1976).
[7] D. L. Yeager, J. A. Nichols, and J. T. Golob, J. Chem. Phys. **100**, 6514 (1994).
[8] R. Rydberg, Z. Phys. **76**, 226 (1932).
[9] O. Klein, Z. Phys. **76**, 226 (1932).
[10] A. L. Rees, Proc. Phys. Soc. (London) **59**, 988 (1947).
[11] J. T. Vanderslice, E. A. Mason, W. G. Maish, and E. Lippincott, J. Mol. Spectrosc. **3**, 17 (1959).
[12] Y. Lu, T. Matsui, K. Tanaka, K. Ito, T. Hayaishi, and Y. Morioka, J. Phys. B **25**, 5101 (1992).
[13] Y. Lu, Y. Morioka, T. Matsui, T. Tanaka, H. Yoshii, R. I. Hall, T. Hayaishi, and K. Ito, J. Chem. Phys. **102**, 1553 (1995).
[14] K. Ito, Y. Morioka, M. Ukai, N. Kouchi, Y. Hatano, and T. Hayaishi, Rev. Sci. Instrum. **66**, 2119 (1995).
[15] P. H. Krupenie, J. Phys. Chem. Ref. Data **1**, 423 (1972).
[16] G. L. Bhale and P. R. Rao, Proc. Indian Acad. Sci. Sect. A **67**, 350 (1968).
[17] K. P. Huber and G. Herzberg, *Molecular Spectra and Molecular Structure*, Constants of Diatomic Molecules, Volume IV (Van Nostrand, New York, 1974).
[18] R. J. Le Roy, Mol. Specrosc. **1**, 113 (1973).
[19] R. B. Singh and D. R. Rai, J. Mol. Specrosc. **19**, 424 (1966).
[20] T. E. Nevin, Proc. R. Soc. London **174**, 371 (1940).
[21] A. Tabché-Fouhaillé, J. Durup, J. T. Moseley, J. B. Ozenne, C. Pernot, and M. Tadjeddine, Chem. Phys. **17**, 81 (1976).
[22] J. T. Moselev, M. Tadjeddine, J. Durup, J. B. Ozenne, C. Pernot, and A. Tabché-Fouhaillé, Phys. Rev. Lett. **37**, 891 (1976).
[23] M. Tadjeddine, R. Abouaf, P. C. Cosby, B. A. Huber, and J. T. Moseley, J. Chem. Phys. **69**, 710 (1978).
[24] J. T. Moseley, P. C. Cosby, J. B. Ozenne, and J. Durup, J. Chem. Phys. **70**, 1474 (1979).
[25] A. Carrington, P. G. Roberts, and P. J. Sarre, Mol. Phys. **34**, 291 (1977).